

1 **Monitoring climate sensitivity shifts in tree-rings of eastern boreal North America using model-**
2 **data comparison**

3

4 Clémentine Ols^{1,2*}, Martin P. Girardin³, Annika Hofgaard⁴, Yves Bergeron¹ & Igor Drobyshev^{1,5}

5 1- Institut de recherche sur les forêts, Université du Québec en Abitibi-Témiscamingue, 445
6 boul. de l'Université, Rouyn-Noranda, QC J9X 5E4, Canada

7 2- Institut National de l'Information Géographique et Forestière, Laboratoire d'Inventaire
8 Forestier, 14 rue Girardet, 54000 Nancy, France

9 3- Natural Resources Canada, Canadian Forest Service, Laurentian Forestry Centre, 1055 du
10 P.E.P.S. P.O. Box 10380, Stn. Sainte-Foy, Quebec, QC G1V 4C7, Canada

11 4- Norwegian Institute for Nature Research, P.O. Box 5685 Sluppen, NO-7485 Trondheim,
12 Norway

13 5- Southern Swedish Forest Research Centre, Swedish University of Agricultural Sciences, P.O.
14 Box 49, SE-230 53 Alnarp, Sweden

15

16 Clementine Ols, *Corresponding author, (1) clementine.ols@ign.fr, (2) clementine.ols@uqat.ca, :
17 +33782818920

18 Martin P. Girardin, martin.girardin@canada.ca

19 Annika Hofgaard, annika.hofgaard@nina.no

20 Yves Bergeron, yves.bergeron@uqat.ca

21 Igor Drobyshev, (1) igor.drobyshev@uqat.ca, (2) igor.drobyshev@slu.se

22 For author contributions see footnote below¹

23

24 Keywords: boreal forests, North America, bioclimatic models, climate change, climate-growth
25 relationships, black spruce, *Picea mariana*

C.O., M.P.G. and I.D. designed research; C.O. and M.P.G. performed research; C.O. and M.P.G. contributed new reagents/analytic tools; C.O. and M.P.G. analyzed data; and C.O., M.P.G., I.D., A.H., and Y.B. wrote the paper.

Shifts in tree growth sensitivity to climate

26 Abstract

27 The growth of high-latitude temperature-limited boreal forest ecosystems is projected to become more
28 constrained by soil water availability with continuing warming. The purpose of this study was to
29 document [ongoing shifts in tree growth sensitivity](#) to the evolving local climate in unmanaged black
30 spruce (*Picea mariana* (Mill) B.S.P.) forests of eastern boreal North America [49°N-52°N, 58°W-
31 82°W] using a comparative study of [field](#) and modeled data. We investigated growth relationships to
32 climate (gridded monthly data) from observed (50 site tree-ring width chronologies) and simulated
33 growth data (stand-level bioclimatic model) over 1908-2013. No clear strengthening of water control
34 upon tree growth in recent decades was detected. Despite climate warming, photosynthesis (main
35 driver of bioclimatic models) and xylem production (main driver of radial growth) have remained
36 temperature-limited. Analyses revealed, however, [a weakening of the influence of growing season
37 temperature on growth](#) during the mid- to late-20th century in observed data, particularly at high-
38 latitude (> 51.5°N) mountainous sites. This divergence was absent from simulated data which resulted
39 in a clear model-data desynchronization. [Thorough investigations revealed that both phenomena were
40 mostly linked to the quality of climate data, precipitation data being of particular concerns. The scarce
41 network of weather stations over eastern North America affects the accuracy of local climate
42 variability and critically limits our ability to monitor climate change impacts on high-latitude
43 ecosystems while drought severity is projected to rise. Climate estimates from remote sensing could
44 help address some of these issues in the future.](#)

45

46 **Introduction**

47 [Tree growth rates are well correlated with spatial and temporal climate variability](#) (Gifford and
48 Evans 1981; Rennenberg and others 2006; Wu and others 2012; Vlam and others 2014; Gricar and
49 others 2015). During the last century, increasing anthropogenic activities have altered global climate
50 and local weather dynamics (Mann and others 1998; IPCC 2014), thereby affecting tree growth
51 processes. [Tree growth in many boreal regions lost its positive response to rising temperatures during](#)
52 [the late-20th century](#) (D'Arrigo and others 2008), [a phenomena often in parallel with increased](#)
53 [sensitivity of tree growth to precipitation and drought severity](#) (Buermann and others 2014; Galván
54 and others 2015; Latte and others 2015). But causes for [changing](#) climate sensitivity in tree-rings vary
55 and may also result from responses to other phenomena associated with changing cloud cover, delayed
56 snowmelt and increasing local pollution (Vaganov and others 1999; D'Arrigo and others 2008).
57 Furthermore, links between temporal variations in tree responses to climate and climate change likely
58 involve [cross-scale](#) interactions between abiotic and biotic variables, e.g., tree age/size and site
59 characteristics effects on tree growth (Carrer and Urbinati 2004; Rossi and others 2008; Ibáñez and
60 others 2014; Navarro-Cerrillo and others 2014) and insect herbivory (Krause and others 2012;
61 Fierravanti and others 2015). The evaluation of climate change impacts on tree growth dynamics
62 remains challenging (Girardin and others 2016b).

63 [In the boreal forest of eastern North America](#), seasonal temperatures have increased by as much
64 as 3°C since the beginning of the 20th century (Hansen and others 2010; Jaume-Santero and others
65 2016), while [seasonal precipitation](#) have shown variable patterns (Wang and others 2014). Studies
66 have reported a decrease in tree growth [sensitivity to growing season temperature at historically](#)
67 [‘temperature-limited’ high latitude and high altitude forests](#) (Jacoby and D'Arrigo 1995; Briffa and
68 others 1998; Galván and others 2015). In parallel, growth declines have been reported during the late
69 20th century (Girardin and others 2016a) and occurrence of [years with extremely low growth](#) in the
70 [boreal forest of eastern North America](#) has increased over the 20th century (Ols and others 2016). [Both](#)
71 [phenomena have been attributed to increased drought impacts on tree growth](#). Projections [have shown](#)
72 that during the next century, soil water availability, [atmospheric water demand](#) and heat stress in the
73 [boreal forest of eastern North America will increasingly limit](#) tree growth as a consequence of the

74 continuing warming (Girardin and others 2016b; Novick and others 2016). The degree to which this
75 forest will adapt to warmer and drier conditions, e.g. by increasing their water use efficiency, is
76 uncertain (Charney and others 2016). It is, therefore, important that these ecosystems are continuously
77 monitored to detect early warning signs of changes in climatic controls of tree growth (Gauthier and
78 others 2015). However, such an observation-based monitoring is complicated by the large spatial
79 extent of the boreal forest of eastern North America and by the multiple species involved.

80 Forest growth models facilitate the exploration of tree growth processes and their expected
81 relationship to the evolving local climate. Such a bioclimatic model can be built upon sets of
82 mathematical equations accounting for non-linear relationships between specific environmental and
83 physiological variables derived from empirical observations (Landsberg and Waring 1997; Misson
84 2004). Studying the coherency in climatic signals contained in empirical tree growth data and
85 simulated tree-growth data may help understand whether variations in tree-growth responses to
86 climate emerge from changing climate alone or from changes in tree-growth sensitivity to climate.
87 Modelling may also help studying tree growth and its sensitivity to climate in areas where ground
88 sampling is more difficult due to the remoteness of locations and costs associated with this type of
89 sampling.

90 In this study, we explore the possibilities of monitoring shifts in tree growth sensitivity to climate
91 in boreal black spruce forests in eastern North America by comparing observed and model-based
92 climate-growth relationships over 1908-2013. Observed data consisted of a newly acquired network of
93 50 annually resolved and absolutely dated black spruce tree-ring width chronologies covering
94 latitudinal and longitudinal gradients of eastern boreal North America [49°N-52°N, 58°W-82°W, Fig.
95 1]. As for the model-based data, we used a stand-level bioclimatic model, based on the Physiological
96 Principle Predicting Growth (3PG) model (Landsberg and Waring 1997), to simulate yearly site-
97 specific net primary production (NPP) for the period encompassing observed data (i.e. 1908-2013).
98 Two hypotheses were formulated on the basis of the widely accepted evidence that temperatures have
99 been rising in the study region:

Shifts in tree growth sensitivity to climate

100 (H1) Yearly variability in tree growth is under the control of climate. The validity of this
101 hypothesis implies a significant correlation between tree-ring width data and climatically driven
102 simulations of NPP;

103 (H2) The control of water on tree growth has increased over time along with the rise of
104 temperature, particularly at high-latitude and high-altitude forests. This implies an increased positive
105 sensitivity to precipitation both in tree-ring width data and climatically driven simulations of NPP.

106

107 **Material and methods**

108 *Study area*

109 The study area consists of three latitudinal transects (western, central and eastern; Fig. 1a) established
110 in northern boreal Quebec (Ols and others 2016). The topography in this area is characterized by low
111 plains in the west (200-350 m above sea level [a.s.l.]) and by mountains, particularly pronounced in
112 the north, central and eastern regions (up to 1128 m a.s.l. in the Otish Mountains). The two main
113 climatic gradients in the study area are a decreasing temperature gradient from south to north and an
114 increasing summer (June to August) precipitation gradient from west to east (Fig. 1b). The eastern
115 region is regularly prone to spruce budworm outbreaks (Boulanger and Arseneault 2004).

116

117 *Tree-ring width measurements*

118 Tree-growth data (n= 890 trees) were collected at 50 sites located along the three latitudinal transects
119 (Fig. 1a, Table S1) (Ols and others 2016). All sites were unmanaged old-growth pure black spruce
120 (*Picea mariana* (Mill) B.S.P.) forests growing on xeric to meso-xeric soils (Direction des inventaires
121 forestiers 2015). Between 10 and 27 dominant trees (standing living or dead) were sampled per site
122 (one core per tree). Sampled cores were processed using standard procedures and rings were visually
123 cross-dated prior to measuring. Tree-ring width measurements were detrended using a 60-yr spline to
124 eliminate noise caused by site- and biological-related effects (e.g. competition, self-thinning and
125 aging) (Cook and Peters 1997). Detrended ring-width measurements were then processed using
126 autoregressive modeling to remove autocorrelation (pre-whitening) and averaged into site-specific
127 residual tree-ring width (RWI) chronologies using a robust bi-weighted mean.

128

129 *Climate data*

130 Climatological data used as input for the bioclimatic model and in the calculations of climate-growth
131 relationships were monthly means of maximum (Tmax) and minimum (Tmin) temperatures, and
132 monthly total precipitation (Prec), all extracted from the 0.5° x 0.5° CRU TS 3.22 database (Harris and
133 others 2014). The climatic characteristics of each study site were extracted over the 1901-2013 period,
134 using a site-centered 0.5° x 0.5° grid cell. We retrieved data from twenty-one grid cells, with each grid
135 cell containing between 1 and 7 study sites. Consequently, some study sites presented identical
136 climatic characteristics (Table S1). To test the influence of climate data type on model simulations and
137 climate-growth relationships, site-specific climate data (Tmin, Tmax and Prec) were also extracted
138 [over the 1901-2013 period](#) (using the same procedures as above) from three alternative databases: (1)
139 the Canadian software BioSIM (Régnière and others 2014), (2) the combined 0.5° x 0.5° CRU TS 3.22
140 temperature (Harris and others 2014) and GPCC precipitation (Full Data Reanalysis Version 7)
141 (Schneider and others 2015), and (3) Twentieth Century Reanalysis (20CR) (Compo and others 2011)
142 datasets. The 20CR data are derived from oceanic temperature and surface pressure data, and do not
143 incorporate precipitation and station temperature records (Compo and others 2011); 20CR may thus be
144 viewed as independent from all other climate products.

145 The boreal region of eastern Canada is not covered by a dense network of weather stations
146 (Fig. S1). In many instances, the existing stations have been running intermittently (Girardin and
147 others 2016b). To capture precipitation and temperature input data accuracy through space and time,
148 the number and location of meteorological stations used for climatic interpolations within our study
149 area were extracted. We also extracted the only long-running hydrological record of the study area: the
150 1960-1993 De Pontois river flow [from HYDAT 28.0](#) ([Water Survey of Canada](#),
151 <http://www.ec.gc.ca/rhc-wsc>) (Table S3) , and used this record as a surrogate for drought conditions
152 (Haslinger and others 2014).

153

154 *Forest attributes*

Shifts in tree growth sensitivity to climate

155 Biometric information necessary for the model simulation was obtained as follows. First, the above-
156 ground biomass in mega-grams per hectare (W_{abg}) was estimated at each study site using country-
157 wide species-specific allometric equations (Paré and others 2013) applied to site-specific basal area
158 (Table S2). Site-specific topography data (slope and aspect values; Table S2) were then extracted from
159 Canada 3D, a digital elevation model produced by the Canadian Forestry Service (Natural Resources
160 Canada 2002) using the ArcGIS® software (ESRI 2011). Finally, historical patterns of defoliation
161 severity by the spruce budworm (1967–2016), compiled from Quebec’s provincial annual surveys
162 (Ministère des Forêts, de la Faune et des Parcs du Québec (MFFPQ) 2014), were extracted for each of
163 our sites.

164

165 *Net primary productivity data*

166 Net primary production (NPP) at our 50 sites was simulated using the StandLEAP model (version 0.1
167 SVN) (Girardin and others 2016b). StandLEAP is a generalized plot-level model based on the 3PG
168 model (Landsberg and Waring 1997) that is applicable to relatively homogeneous forests. [It was
169 developed for the estimation of forest productivity over large areas \(e.g. Girardin and others 2016b\)
170 but with a spatial resolution sufficiently fine for forest management \(e.g. Raulier and others 2000;
171 Coulombe and others 2009; Anyomi and others 2014\).](#) StandLEAP can be parameterized for
172 individual species and its application to any stand does not require fine-tuning of the model to fit the
173 data. [The model has been tested against numerous independent tree-ring datasets in western, central
174 and eastern Canada \(Girardin and others 2008, 2011b, 2011a, 2012, 2014, 2016b\).](#) In StandLEAP,
175 parameters are set up to fully characterize the impact of many interacting and non-linear modifiers of
176 carbon flux quantities (e.g. growth and respiration). Absorbed photosynthetically active radiation
177 (APAR) is related to growth primary production (GPP) using a radiation use efficiency (RUE)
178 coefficient that differs among locations and through time as a function of environmental constraints.
179 Constraints take the form of species-specific parameters ($f_1 \dots f_n$) that take on a value of 1 under
180 average conditions; they are closer to zero to represent increasing limitations, or above 1 as conditions
181 improve towards optimum. [Constraints represent the impact of soil drought \(Bernier and others 2002\),
182 frost \(Aber and others 1996\) \(both limited to a maximum of 1.0\), mean maximum and minimum daily](#)

Shifts in tree growth sensitivity to climate

183 air temperature, vapor pressure deficit (VPD), monthly radiation, and leaf area index (where values
184 greater than 1.0 are possible) on GPP. The following equation summarizes these functions:

$$185 \quad GPP = APAR \times (\overline{RUE} \times f_1 f_2 \dots f_n), \quad (1)$$

186 where \overline{RUE} represents a species-specific mean value of RUE applicable to the entire species' range.

187 Canopy light absorption and photosynthesis parameters were derived from metadata generated using a
188 more detailed multi-layer, hourly time-step model of canopy photosynthesis and transpiration called
189 FineLEAP (Raulier and others 2000; Hall and others 2006). Representation of photosynthesis in
190 FineLEAP is based on the equations of Farquhar and others (1980). Additional details of the
191 procedure and origin of the basic field measurements and procedure for estimation of parameters for
192 radiation interception, radiation- and water-use-efficiency can be found in Hall and others (2006). NPP
193 is computed monthly, after partitioning respiration into maintenance (R_m) and growth (R_g: a fixed
194 proportion of the difference between GPP and R_m) quantities and subtracting these from GPP.
195 Maintenance respiration is computed as a function of temperature using a Q₁₀ relationship (Ågren and
196 Axelsson 1980; Ryan 1991; Lavigne and Ryan 1997). Acclimation of respiration to temperature is
197 modelled using the equation of Smith and others (2016). As in 3-PG, part of NPP is first allocated to
198 fine roots (Eq. (13) in Landsberg and Waring 1997) on a yearly basis and then to replacement of
199 carbon biomass lost to leaf and fine woody litter turnover. The remaining NPP is then allocated to
200 increments in stand carbon compartments of foliage, branches, coarse roots and stems. The modifier
201 for soil water availability is based on modeled water balance coupled with transpiration and NPP, as
202 described by Bernier and others (2002). The impact of CO₂ fertilization is included through a modifier
203 of the potential water use efficiency, as described by Girardin and others (2016b). The active soil
204 depth was set to 600mm at all sites (Table S2). An active soil depth between 300 and 900mm has
205 generally been accepted as a desirable range for black spruce (Viereck and Johnston 1990; Girardin
206 and others 2016b). Three sites (namely, 39, 45 and 47, Table S2) had their above-ground biomass
207 truncated to a maximum value of 110 Mg/ha, because of estimated field values reaching higher than
208 typical conditions for which the model was calibrated. StandLEAP runs on a monthly time-step. All
209 carbon flux quantities used in this study were made insensitive to changing forest age over time, by

Shifts in tree growth sensitivity to climate

210 [fixing constant forest attributes](#) (e.g. biomass and stem densities) across all simulation years. Carbon
211 flux quantities solely express direct climate influences on plant growth, [avoiding the influence of post-
212 fire stand dynamics on fluxes](#) (e.g. Girardin and others 2011a; Pan and others 2011) and allowing a
213 direct comparison with climatically-driven tree-ring width measurements [collected from old-growth
214 forest stands](#). The model does not simulate soil processes other than water balance, since it implicitly
215 assumes constant soil nutrient properties and turnover. [Furthermore, computations assume the absence
216 of insect outbreaks](#).

217

218 *Correlation between tree-ring and NPP metrics*

219 Monthly NPP values obtained from modelling were summed up from July the previous year to June
220 the year of growth, to represent carbon quantities mobilized and allocated to growth from one year to
221 the next (as in Girardin and others 2016b). Carry-over effects from the previous growing season have
222 been reported to [affect significantly](#) tree growth the following season, and particularly in a harsh
223 environment (Babst and others 2014; Ols and others 2016). Lower [carbohydrate reserves](#) the following
224 growing season, can notably decrease the capacity of trees to respond to favorable growth conditions.
225 The correspondence between annual RWI and NPP metrics were then explored through moving
226 correlations (one-sided test) at site level. Correlations were computed in R (R Core Team 2015) using
227 21-yr windows incremented by five years from 1908 to 2013. The null hypothesis of no positive
228 correlation between RWI and NPP was rejected when $p < 0.05$. Temporal stability in correlations
229 between RWI and NPP metrics were also investigated at regional level using the same moving-
230 correlation procedure as above. Regional RWI and NPP metrics were computed as a robust bi-
231 weighted mean of all site-specific metrics. The significance of each 21-yr correlation averaged across
232 sites was evaluated using a competitive test, which combines the probabilities of dependent tests using
233 the Fisher's method (Dai and others 2014). Applied to our specific case, it compares, for each 21-yr
234 period, the distribution of p values of all site-specific NPP and RWI correlations to the distribution of
235 randomly selected 100,000 vectors of p values of similar length. Competitive tests were computed in
236 R using the *competitive.test* function available in the *CombinePValue* package (Dai 2014).

237

238 *Climate-growth relationships*

239 Coherency in the climatic signals contained in RWI and NPP metrics were investigated by correlation
240 analyses. First, correlations between tree-growth metrics and monthly climate data were computed
241 using 21-yr windows incremented by five years from 1908 to 2013 using the *treeclim* package (Zang
242 and Biondi 2015). Climate data included monthly maximum and minimum temperatures and monthly
243 total precipitation. Months spanned from May the previous year to August the year of growth. Site-
244 specific moving correlations were then averaged across all sites to characterize monthly climate-
245 growth relationships at the scale of our study area. The following hypotheses, based on the earlier
246 work by Girardin and others (2016b), were postulated and tested using one-sided tests: (1) growth is
247 positively correlated with previous year September through current year May (hereafter September-
248 May) temperatures, (2) growth is negatively correlated with June-August temperatures, and (3) growth
249 is positively correlated with precipitation, regardless of the month. Alternatively, we also tested the
250 inverse versions of hypotheses 1 to 3: growth is (4) negatively correlated with September-May
251 temperatures, (5) positively correlated with June-August temperatures, and (6) negatively correlated
252 with precipitation. Hypotheses 1-6 were considered true both for months of the previous and current
253 growing season year. These procedures were run both for RWI and NPP series. Note that stronger
254 correlations observed with NPP can logically emerge from computation alone, since NPP is itself
255 computed from these climate data. The significance of each 21-yr correlation averaged across sites
256 was evaluated using the competitive test described earlier. We opted for six one-sided hypotheses
257 instead of three two-sided hypotheses because under two-sided testing the meta-analysis is particularly
258 sensitive when both strong positive and negative effects occur across sites (Whitlock 2005). Finally,
259 the distributions of site-specific correlations with monthly climate variables of the two metrics were
260 compared using the Wilcoxon-Mann-Whitney and Kolmogorov-Smirnov tests.

261

262 **Results**

263 *Climate sensitivities in tree growth metrics*

264 RWI was generally positively correlated with current year spring and summer temperatures (Fig. 2a).
265 However, these correlations decreased substantially and became non-significant during the mid- to

266 late-20th century (Fig. 2a). This decrease in correlation corresponded with the emergence of significant
267 negative correlations with previous summer and previous October temperatures (maximums and
268 minimums) from the 1940s to 1990s, and with current spring precipitation during a brief period
269 covering the 1960-80s (Fig. 2a). In addition, significant positive correlations between RWI and early
270 winter temperatures were observed during the late-20th century (Fig. 2a). The correlation between
271 RWI metrics and De Pontois summer (mean June to August) river flow of the year prior to growth,
272 and over 1960-1993, was significantly positive (median correlation of 0.31), especially at high
273 latitudes (>51.5°N) (Fig. 3). In summary, annual growth variability in this boreal region of eastern
274 North America has shifted from being positively correlated with growing-season temperature early in
275 the 20th century, to being negatively correlated with summer temperature during the mid-century, and
276 then back to being positively correlated with temperature during the late-20th century. There was no
277 clear evidence of a strengthening of tree growth sensitivity to precipitation throughout the 1908-2013
278 period, using CRU precipitation data (Fig. 2a).

279 Relationships between NPP and monthly climate variables were similar to those observed for
280 RWI metrics (Fig. 2b, c). NPP correlated positively with current year temperatures, but this
281 relationship was much weaker from 1958 to 1988 (Fig. 2b). Between 1973 and 1998 there was an
282 emergence of significant negative correlations with previous summer temperature (Fig. 2b). Unlike
283 with RWI, there was a period of sustained significant positive correlations with July or August
284 precipitation during the year contemporaneous to growth from 1933 to 1998 (Fig. 2b). Wilcoxon-
285 Mann-Whitney tests indicated that the distribution of correlations between NPP and monthly
286 temperature (minimum and maximum) was generally more homogeneous than with RWI (Fig. 2c). By
287 contrast, the distributions of correlations to precipitation for both metrics were mostly similar. This
288 was also observed using the Kolmogorov-Smirnov test (Fig. S2). NPP metrics and De Pontois summer
289 river flow were not significantly correlated ($p > 0.05$) (data not shown). However, these variables were
290 significantly correlated after a first-difference transformation in 33 of the 50 study sites, mostly north
291 of 51.5°N and west of 74.0°W (median correlation of 0.32; correlation pattern similar to the RWI
292 pattern presented in Fig. 3d but with both variables taken on their non-lagged calendar years; results
293 not shown). In summary, NPP variability shifted from being temperature-driven in the early-20th

Shifts in tree growth sensitivity to climate

294 century (an indication of temperature limitation on the rate of photosynthesis), to precipitation-driven
295 during the mid- to late-20th century (i.e. the influence of available moisture), and then again
296 temperature-driven during the late-20th century.

297

298 *Synchronicity in tree growth metrics*

299 Correlations between site-specific RWI and NPP metrics at regional level were often positive and
300 significant during the early-20th century and throughout the late-20th to early-21st centuries (Fig. 4).
301 However, a clear desynchronization was observed in the middle of the century at almost all sites, when
302 correlations substantially decreased to become negative and occasionally significantly negative (Fig.
303 5, left-hand panels). Although its duration and timing differed across sites, this desynchronization was
304 most prominent in mountainous north easternmost sites (Fig. 6d), i.e. in areas ongoing the most rapid
305 warming (Fig. 1a). First-differencing (subtraction of the value at year_t by the value at year_{t-1}) of the
306 RWI and NPP data enhanced correlations during the late-20th century but decreased correlations
307 during the early-20th century across the whole area (Fig. 5, right-hand panels). It is noteworthy that the
308 same mid- to late-20th century desynchronization between observed and simulated tree-growth metrics
309 was obtained using alternative climate datasets, albeit there were variations in the onset and duration
310 of this desynchronization depending on the data products (Fig. S3). For instance, correlations between
311 NPP and RWI were improved during the 1933-1963 period when fed by simulations of the NPP
312 driven by the 20CR data, albeit it did not fully compensate for model-data desynchronization (Fig.
313 S3d).

314

315 **Discussion**

316 The purpose of this study was to document shifts in tree growth sensitivity to climate in temperature-
317 limited boreal forest ecosystems of eastern boreal North America over 1908-2013 using a comparative
318 study of field and modeled data.

319 Despite climate warming in the study area (Figs. 1a and S4), there was no clear evidence for a
320 strengthening of radial tree growth (RWI) sensitivity to precipitation during recent decades (Fig. 2).

321 The post-1980 significant positive correlations between (1) growing-season temperature and radial

Shifts in tree growth sensitivity to climate

322 growth (Fig. 2c), and between (2) radial growth and modeled productivity (NPP) across the entire
323 study region (Fig. 4) indicate that both photosynthesis (the main driver of the model) and xylem
324 formation (the main driver of radial growth) have until recently remained temperature-limited. This
325 contradicts earlier findings reporting the strengthening of soil water availability control on tree growth
326 in the boreal forest of eastern North America over the 20th century (see Introduction). The response of
327 tree radial growth in our studied regions is therefore different from the response frequently reported in
328 the literature for the boreal forest. A likely reason for this lack on increased sensitivity of tree growth
329 to precipitation may be that, despite rising temperature (Fig. 1a), the atmospheric water demand may
330 have decreased over the course of the 20th century in our study area (Fig. S5; also see Fig. S9 in
331 Girardin and others 2016b). A decrease in water demand, coupled with a potential increase in water
332 use efficiency under elevated atmospheric CO₂ concentrations, may have contributed to the
333 stabilization of tree dependence on incoming precipitation necessary for soil water recharge.

334 Our results revealed that while modeled productivity remained somewhat spring temperature
335 sensitive over the entire study period, the positive influence of growing season temperature on radial
336 growth disappeared. This phenomenon occurred in parallel with an increased sensitivity to moisture,
337 as indicated by the negative correlation between radial growth and summer temperature, by the
338 positive correlation between radial growth and the De Pontois summer river flow, and by the positive
339 correlation between modeled productivity and July precipitation. However, during this same period
340 the overall region-wide significant synchrony between modeled productivity and radial growth also
341 dropped to become insignificant, particularly at eastern high-latitude mountainous sites, i.e. those
342 undergoing the strongest warming (Fig. 1a). These sudden model-data desynchronization is
343 noteworthy and deserves attention, as it may impair our capacity to monitor shifts in tree growth
344 sensitivity to climate in these forests. Below we discuss three factors that may be involved in this
345 desynchronization: accuracy of input climate data, the advent of external factors in the ecosystem, and
346 model uncertainties.

347 Climate data uncertainties have a large influence on model-based estimations of historical and
348 ongoing ecosystem processes: the choice of climate dataset, with those of precipitation being of
349 particular concern, affects the capacity to identify drivers of variability in empirical data products and

350 [model results](#) (e.g. Daly and others 1994; Ito and others 2017; Wu and others 2017). For example, the
351 probability of a false negative result (e.g. a significant RWI-precipitation correlation not detected
352 when a true relationship exists) could theoretically be higher at sites where climate data quality is
353 lowest (Wilson and others 2007). [In the current study, the quality of climate data is likely to be a](#)
354 [critical factor explaining the drop in model-data correspondence](#) during the mid- to late-20th century.
355 First, the desynchronization in model-data correspondence was most prominent at sites located above
356 51.5°N (Fig. 5c), that is, where station density is low (Figs. 5 and S1). There is, therefore, an apparent
357 relationship between station density and climate signal degradation.

358 Additionally, weak model-data correspondence was clearly linked to altitudinal differences
359 between reference stations (mainly located along the coast) and mountainous sampled sites, with a
360 higher capacity to detect a positive correlation between radial growth and modeled productivity at low
361 altitude sampling locations (Fig. 6d). [This bias finds explanation in the fact that CRU temperature](#)
362 [interpolations over boreal eastern North America do not depict altitudinal climate gradients \(Fig. S6\).](#)
363 [Our capacity to model forest growth in mountainous regions is hence very likely hindered by](#)
364 [inaccuracies of temperature and precipitation estimates at these high-altitude sites. The variations in](#)
365 [the onset and duration of the desynchronization between radial growth and modeled productivity](#)
366 [across climate data products illustrate the problem of climate data uncertainties.](#) Noteworthy is that the
367 onset of the desynchronization between radial growth and modeled productivity coincides with a
368 period of high weather station density in the region (Figs. 6a and S1b&c) but also of [high uncertainty](#)
369 [in estimates of precipitation data in the region \(Figs. S1c and S7\).](#) Indeed, cross-correlations between
370 [CRU and the 20th Century Reanalysis \(20CR\) gridded data show a strong inconsistency during the](#)
371 [period 1940-1980 \(Fig. S7\), a sign of significant error in the estimation of climatic data either in one](#)
372 [or the other climatic product.](#)

373 Last, the formulation of the model used herein may be missing important dynamic processes
374 associated with insect outbreaks, carbohydrate mobilization and storage, snow accumulation and
375 thawing, initiation of leaf-out and growth processes.

376 Notably, outbreaks of the eastern spruce budworm, regular in the boreal forest of eastern North
377 America, could have contaminate field data by disrupting radial growth responses to local climate and

Shifts in tree growth sensitivity to climate

378 caused the model-data desynchronization (Girardin and others 2016b), simulations being computed in
379 an outbreaks-free environment. However, we did not observe any obvious abrupt growth decline or
380 release, typical of severe outbreak defoliation on these site chronologies (Figs. 4 and S7). Also, most
381 of the sites showing desynchronization were located in an area that did not show historical evidence of
382 spruce budworm outbreaks during the 1947-1958, 1975-1992 and 2007-2016 periods (Fig. 6b).
383 Furthermore, the sampled stands were free of the main budworm host-species *Abies balsamea*.
384 Although the influence of such disturbance on growth can not entirely be ruled out, its role on the
385 observed model-data desynchronization can be only minor. It may, however, become an important
386 concern if this experimental design is to be applied in regions where this disturbance is recurrent
387 (Girardin and others 2016b).

388 Our experimental design assumes that radial growth and modeled productivity are directly comparable
389 analogs. This, however, disregards documented evidences that shifts in radial growth sensitivity, to
390 temperature for instance, emerge from changes in allocation of assimilates within a tree (Lapenis and
391 others 2013). Assimilates allocation is strongly sensitive to stand density (e.g. denser stands favoring
392 allocation to terminal buds to increase access to light) and climate (e.g. drier climate favoring
393 allocation to roots to increase access to water). The period of desynchronization was characterized by
394 a decrease in spring precipitation and an increase in spring temperature (Fig. S4). Such climatic
395 conditions may have temporarily favored the allocation of assimilates to the root system against radial
396 growth, disrupting radial growth responses to climate. In a sensitivity analysis in which the total
397 annual productivity data were substituted with the productivity fraction allocated to the stem (as in
398 Girardin and others 2008), we noted an improved model-data correspondence during the first half
399 (1940-1960) of the divergent period (Fig. S9). But the correspondence deteriorated substantially
400 during the second half (1960-1980) (Fig. S9). Moreover, any of the sites showing model-data
401 desynchronization were located in open-canopy stands nearby the limit between the spruce-moss and
402 spruce-lichen domains, located north of 51.5°N (Robitaille and Saucier 1998). Hence there are no
403 reasons to believe that height growth would have been favored against diameter growth during the
404 mid- to late-20th century. Model-data desynchronization during the mid- to late-20th century,
405 therefore, do not appear linked to shifts in field growth allocation patterns.

406 If we do not question the quality of precipitation data, the sudden negative sensitivity to spring
407 precipitation in radial growth over the mid- to late-20th century, not observed with modeled
408 productivity, may be indicative of a stronger negative impact of spring precipitation on tree growth
409 (Huang and others 2010; Girard and others 2011; Ols and others 2016). Sites presenting a sudden
410 negative sensitivity to spring precipitation were the ones undergoing the strongest warming (Fig. 1a)
411 and were mainly located in high-altitude mountainous areas (Fig. 6d). Snow dynamics (fall and
412 melting) influence tree growth and climate-growth relationships at boreal latitudes (Frechette and
413 others 2011; David 2015), particularly along altitudinal gradients (Trujillo and others 2012). Notably,
414 a thick spring snow cover may delay the start of the growing season through delayed snow melt
415 (Vaganov and others 1999). The current model formulation does not include a dynamic snow model,
416 as in Terrier and others (2013). This may mislead the onset and duration of the drought season and
417 ultimately affect the capacity to uncover drivers associated with the water balance at high-altitude
418 sites.

419

420 **Conclusion**

421 Climate change and its impact on high-latitude boreal ecosystems are now recognized. There is no
422 doubt that, in the near future, intensive efforts will need to be taken to monitor these impacts in order
423 to pave the way for adaptation and mitigation solutions (Gauthier and others 2015). This will require
424 tools to adequately link ecosystem dynamics to atmospheric properties. In this view, we showed that
425 bioclimatic models can track fairly well processes leading to forest growth variability of the
426 northernmost boreal forest of eastern North America through space and time when growth remains
427 temperature-limited (Girardin and others 2008, 2016b). Our work nevertheless illustrated some of the
428 challenges that hinder the capacity to keep monitoring high-latitude boreal ecosystems at fine-scale
429 across a diversity of landscapes. Among issues, uncertainties in climate data are of particular concern.
430 Many of the temperature-limited regions of boreal Canada are covered by a scarce network of weather
431 stations, which affects accuracy of local climate variability estimates and make it difficult to relate
432 climate to ecosystems' dynamics. Availability of climate data may, therefore, critically limit our
433 ability to monitor climate change impacts on high-latitude forest ecosystems while drought severity is

Shifts in tree growth sensitivity to climate

434 projected to rise. Recent estimates of climate data, notably of precipitation and snow cover, through
435 remote sensing could help address some of these issues in the future.

436

437 Acknowledgements

438 We are thankful to Emeline Chaste for GIS analyses and to Xiao Jing Guo for assistance with
439 StandLEAP. This study was funded by the Natural Sciences and Engineering Research Council of
440 Canada (NSERC Strategic and Discovery Grants), by the Nordic Forest Research Cooperation
441 Committee (SNS), by the Canadian Forest Service and by the Research Council of Norway (grant
442 160022/E50). This work was also supported by a fellowship from the Forest Complexity Modelling
443 program. Authors do not present any conflicts of interests.

444 **References**

- 445 Aber JD, Reich PB, Goulden ML. 1996. Extrapolating leaf CO₂ exchange to the canopy: a generalized
446 model of forest photosynthesis compared with measurements by eddy correlation. *Oecologia*
447 106:257–65.
- 448 Ågren GI, Axelsson B. 1980. Population respiration: A theoretical approach. *Ecol Model* 11:39–54.
- 449 Anyomi KA, Raulier F, Bergeron Y, Mailly D, Girardin MP. 2014. Spatial and temporal heterogeneity
450 of forest site productivity drivers: a case study within the eastern boreal forests of Canada.
451 *Landsc Ecol* 29:905–18.
- 452 Babst F, Bouriaud O, Papale D, Gielen B, Janssens IA, Nikinmaa E, Ibrom A, Wu J, Bernhofer C,
453 Kostner B, Grunwald T, Seufert G, Ciais P, Frank D. 2014. Above-ground woody carbon
454 sequestration measured from tree rings is coherent with net ecosystem productivity at five
455 eddy-covariance sites. *New Phytol* 201:1289–303.
- 456 Bernier PY, Bréda N, Granier A, Raulier F, Mathieu F. 2002. Validation of a canopy gas exchange
457 model and derivation of a soil water modifier for transpiration for sugar maple (*Acer*
458 *saccharum* Marsh.) using sap flow density measurements. *For Ecol Manag* 163:185–96.
- 459 Boulanger Y, Arseneault D. 2004. Spruce budworm outbreaks in eastern Quebec over the last 450
460 years. *Can J Res* 34:1035–43.
- 461 Briffa KR, Schweingruber FH, Jones PD, Osborn TJ, Shiyatov SG, Vaganov EA. 1998. Reduced
462 sensitivity of recent tree-growth to temperature at high northern latitudes. *Nature* 391:678–82.
- 463 Buermann W, Parida B, Jung M, MacDonald GM, Tucker CJ, Reichstein M. 2014. Recent shift in
464 Eurasian boreal forest greening response may be associated with warmer and drier summers.
465 *Geophys Res Lett* 41:1995–2002.
- 466 Carrer M, Urbinati C. 2004. Age-dependent tree-ring growth responses to climate in *Larix decidua* and
467 *Pinus cembra*. *Ecology* 85:730–40.
- 468 Charney ND, Babst F, Poulter B, Record S, Trouet VM, Frank D, Enquist BJ, Evans ME. 2016.
469 Observed forest sensitivity to climate implies large changes in 21st century North American
470 forest growth. *Ecol Lett*. <http://www.ncbi.nlm.nih.gov/pubmed/27434040>

Shifts in tree growth sensitivity to climate

- 471 Compo GP, Whitaker JS, Sardeshmukh PD, Matsui N, Allan RJ, Yin X, Gleason BE, Vose RS,
472 Rutledge G, Bessemoulin P, Brönnimann S, Brunet M, Crouthamel RI, Grant AN, Groisman
473 PY, Jones PD, Kruk MC, Kruger AC, Marshall GJ, Maugeri M, Mok HY, Nordli Ø, Ross TF,
474 Trigo RM, Wang XL, Woodruff SD, Worley SJ. 2011. The Twentieth Century Reanalysis
475 Project. *Q J R Meteorol Soc* 137:1–28.
- 476 Cook ER, Peters K. 1997. Calculating unbiased tree-ring indices for the study of climatic and
477 environmental change. *Holocene* 7:361–70.
- 478 Coulombe S, Bernier PY, Raulier F. 2009. Uncertainty in detecting climate change impact on the
479 projected yield of black spruce (*Picea mariana*). *Ecol Manage* 259:730–738.
- 480 Dai H. 2014. CombinePValue: Combine a vector of correlated p-values. R package version 1.0.
481 <http://CRAN.R-project.org/package=CombinePValue>
- 482 Dai H, Leeder JS, Cui Y. 2014. A modified generalized Fisher method for combining probabilities
483 from dependent tests. *Front Genet* 5:32.
- 484 Daly C, Neilson RP, Phillips DL. 1994. A Statistical-Topographic Model for Mapping Climatological
485 Precipitation over Mountainous Terrain. *J Appl Meteorol* 33:140–58.
- 486 D'Arrigo RD, Wilson R, Liepert B, Cherubini P. 2008. On the 'Divergence Problem' in northern
487 forests: A review of the tree ring evidence and possible causes. *Glob Planet Chang* 60:289–
488 305.
- 489 David V. 2015. Remote sensing of interannual boreal forest NDVI in relation to climatic conditions in
490 interior Alaska. *Env Res Lett* 10:125016.
- 491 Direction des inventaires forestiers. 2015. Norme de stratification écoforestière - Quatrième inventaire
492 écoforestier du Québec méridional. Ministère des forêts, de la faune et des parcs
493 <https://www.mffp.gouv.qc.ca/forets/inventaire/pdf/norme-stratification.pdf>. Last accessed
494 09/02/2017
- 495 ESRI. 2011. ArcGIS Desktop: Release 10. Redlands, CA: Environmental Systems Research Institute.
- 496 Farquhar GD, von Caemmerer S, Berry JA. 1980. A biochemical model of photosynthetic CO₂
497 assimilation in leaves of C₃ species. *Planta* 149:78–90.

Shifts in tree growth sensitivity to climate

- 498 Fierravanti A, Coccozza C, Palombo C, Rossi S, Deslauriers A, Tognetti R. 2015. Environmental-
499 mediated relationships between tree growth of black spruce and abundance of spruce
500 budworm along a latitudinal transect in Quebec, Canada. *Agric Meteorol* 213:53–63.
- 501 Frechette E, Ensminger I, Bergeron Y, Gessler A, Berninger F. 2011. Will changes in root-zone
502 temperature in boreal spring affect recovery of photosynthesis in *Picea mariana* and *Populus*
503 *tremuloides* in a future climate? *Tree Physiol* 31:1204–16.
- 504 Galván JD, Büntgen U, Ginzler C, Grudh H, Gutiérrez E, Labuhn I, Camarero JJ. 2015. Drought-
505 induced weakening of growth–temperature associations in high-elevation Iberian pines. *Glob*
506 *Planet Chang* 124:95–106.
- 507 Gauthier S, Bernier P, Kuuluvainen T, Shvidenko AZ, Schepaschenko DG. 2015. Boreal forest health
508 and global change. *Science* 349:819–22.
- 509 Gifford RM, Evans LT. 1981. Photosynthesis, carbon partitioning, and yield. *Annu Rev Plant Physiol*
510 32:485–509.
- 511 Girard F, Payette S, Gagnon R. 2011. Dendroecological analysis of black spruce in lichen—spruce
512 woodlands of the closed-crown forest zone in eastern Canada. *Ecoscience* 18:279–94.
- 513 Girardin MP, Bernier PY, Gauthier S. 2011a. Increasing potential NEP of eastern boreal North
514 American forests constrained by decreasing wildfire activity. *Ecosphere* 2:1–23.
- 515 Girardin MP, Bernier PY, Raulier F, Tardif JC, Conciatori F, Guo XJ. 2011b. Testing for a CO₂
516 fertilization effect on growth of Canadian boreal forests. *J Geophys Res* 116:1–16.
- 517 Girardin MP, Bouriaud O, Hogg EH, Kurz W, Zimmermann NE, Metsaranta JM, de Jong R, Frank
518 DC, Esper J, Buntgen U, Guo XJ, Bhatti J. 2016a. No growth stimulation of Canada’s boreal
519 forest under half-century of combined warming and CO₂ fertilization. *Proc Natl Acad Sci U A*
520 113:E8406–14.
- 521 Girardin MP, Guo XJ, Bernier PY, Raulier F, Gauthier S. 2012. Changes in growth of pristine boreal
522 North American forests from 1950 to 2005 driven by landscape demographics and species
523 traits. *Biogeosciences* 9:2523–2536.

Shifts in tree growth sensitivity to climate

- 524 Girardin MP, Guo XJ, De Jong R, Kinnard C, Bernier P, Raulier F. 2014. Unusual forest growth
525 decline in boreal North America covaries with the retreat of Arctic sea ice. *Glob Change Biol*
526 20:851–66.
- 527 Girardin MP, Hogg EH, Bernier PY, Kurz WA, Guo XJ, Cyr G. 2016b. Negative impacts of high
528 temperatures on growth of black spruce forests intensify with the anticipated climate warming.
529 *Glob Chang Biol* 22:627–43.
- 530 Girardin MP, Raulier F, Bernier PY, Tardif JC. 2008. Response of tree growth to a changing climate
531 in boreal central Canada: A comparison of empirical, process-based, and hybrid modelling
532 approaches. *Ecol Model* 213:209–28.
- 533 Gricar J, Prislán P, de Luis M, Gryc V, Hacurova J, Vavrcik H, Cufar K. 2015. Plasticity in variation
534 of xylem and phloem cell characteristics of Norway spruce under different local conditions.
535 *Front Plant Sci* 6:730.
- 536 Hall RJ, Raulier F, Price DT, Arseneault E, Bernier PY, Case BS, Guo XJ. 2006. Integrating remote
537 sensing and climate data with process-based models to map forest productivity within West-
538 Central Alberta's boreal forest: *Ecoleap-West*. *For Chron* 82:159–76.
- 539 Hansen J, Ruedy R, Sato M, Lo K. 2010. Global surface temperature change. *Rev Geophys* 48.
- 540 Harris I, Jones PD, Osborn TJ, Lister DH. 2014. Updated high-resolution grids of monthly climatic
541 observations --- the CRU TS3.10 dataset. *Int J Clim* 34:623–42.
- 542 Haslinger K, Koffler D, Schöner W, Laaha G. 2014. Exploring the link between meteorological
543 drought and streamflow: Effects of climate-catchment interaction. *Water Resour Res*
544 50:2468–87.
- 545 Huang J-G, Tardif JC, Bergeron Y, Denneler B, Berninger F, Girardin MP. 2010. Radial growth
546 response of four dominant boreal tree species to climate along a latitudinal gradient in the
547 eastern Canadian boreal forest. *Glob Chang Biol* 16:711–31.
- 548 Ibáñez B, Ibáñez I, Gómez-Aparicio L, Ruiz-Benito P, García LV, Marañón T. 2014. Contrasting
549 effects of climate change along life stages of a dominant tree species: The importance of soil-
550 climate interactions. *Divers Distrib* 20:872–83.

Shifts in tree growth sensitivity to climate

- 551 IPCC. 2014. fifth assessment report climate change 2014. synthesis report---summary for
552 policymakers. :1–35.
- 553 Ito A, Nishina K, Reyer CPO, François L, Henrot A-J, Guy Munhoven, Jacquemin I, Tian H, Yang J,
554 Pan S, Morfopoulos C, Betts R, Thomas Hickler, Steinkamp J, Ostberg S, Schaphoff S, Ciais
555 P, Chang J, Rashid Rafique, Zeng N, Zhao F. 2017. Photosynthetic productivity and its
556 efficiencies in ISIMIP2a biome models: benchmarking for impact assessment studies. *Environ*
557 *Res Lett* 12:085001.
- 558 Jacoby GC, D'Arrigo RD. 1995. Tree ring width and density evidence of climatic and potential forest
559 change in Alaska. *Glob Biogeochem Cycles* 9:227–34.
- 560 Jarvis A, Reuter HI, Nelson A, Guevara E. 2008. Hole-filled SRTM for the globe Version 4, available
561 from the CGIAR-CSI SRTM 90m Database. <http://srtm.csi.cgiar.org>
- 562 Jaume-Santero F, Pickler C, Beltrami H, Mareschal J-C. 2016. North American regional climate
563 reconstruction from ground surface temperature histories. *Clim Past* 12:2181–94.
- 564 Krause C, Luszczynski B, Morin H, Rossi S, Plourde P-Y. 2012. Timing of growth reductions in black
565 spruce stem and branches during the 1970s spruce budworm outbreak. *Can J Res* 42:1220–7.
- 566 Landsberg JJ, Waring RH. 1997. A generalised model of forest productivity using simplified concepts
567 of radiation-use efficiency, carbon balance and partitioning. *Ecol Manage* 95:209–28.
- 568 Lapenis AG, Lawrence GB, Heim A, Zheng C, Shortle W. 2013. Climate warming shifts carbon
569 allocation from stemwood to roots in calcium-depleted spruce forests. *Glob Biogeochem*
570 *Cycles* 27:101–7.
- 571 Latte N, Lebourgeois F, Claessens H. 2015. Increased tree-growth synchronization of beech (*Fagus*
572 *sylvatica* L.) in response to climate change in northwestern Europe. *Dendrochronologia*
573 33:69–77.
- 574 Lavigne MB, Ryan MG. 1997. Growth and maintenance respiration rates of aspen, black spruce and
575 jack pine stems at northern and southern BOREAS sites. *Tree Physiol* 17:543–51.
- 576 Mann ME, Bradley RS, Hughes MK. 1998. Global-scale temperature patterns and climate forcing over
577 the past six centuries. *Nature* 392:779–87.

- 578 Ministère des Forêts, de la Faune et des Parcs du Québec (MFFPQ). 2014. Données sur les
579 perturbations naturelles - Insecte : Tordeuse des bourgeons de l'épinette.
580 [https://www.donneesquebec.ca/recherche/fr/dataset/donnees-sur-les-perturbations-naturelles-](https://www.donneesquebec.ca/recherche/fr/dataset/donnees-sur-les-perturbations-naturelles-insecte-tordeuse-des-bourgeons-de-lepinette)
581 [insecte-tordeuse-des-bourgeons-de-lepinette](https://www.donneesquebec.ca/recherche/fr/dataset/donnees-sur-les-perturbations-naturelles-insecte-tordeuse-des-bourgeons-de-lepinette)
- 582 Misson L. 2004. MAIDEN: A model for analyzing ecosystem processes in dendroecology. *Can J Res*
583 34:874–887.
- 584 Natural Resources Canada. 2002. Canada3D, digital elevation model of the Canadian Landmass 30,
585 [http://geogratis.gc.ca/api/en/nrcan-rncan/ess-sst/aa3dc127-4d10-4c1c-a760-](http://geogratis.gc.ca/api/en/nrcan-rncan/ess-sst/aa3dc127-4d10-4c1c-a760-f19bef14042b.html)
586 [f19bef14042b.html](http://geogratis.gc.ca/api/en/nrcan-rncan/ess-sst/aa3dc127-4d10-4c1c-a760-f19bef14042b.html). Government of Canada, Natural Resources Canada, Earth Sciences
587 Sector, Canada Centre for Mapping and Earth Observation, editors.
588 [http://geogratis.gc.ca/api/en/nrcan-rncan/ess-sst/aa3dc127-4d10-4c1c-a760-](http://geogratis.gc.ca/api/en/nrcan-rncan/ess-sst/aa3dc127-4d10-4c1c-a760-f19bef14042b.html)
589 [f19bef14042b.html](http://geogratis.gc.ca/api/en/nrcan-rncan/ess-sst/aa3dc127-4d10-4c1c-a760-f19bef14042b.html)
- 590 Navarro-Cerrillo RM, Sánchez-Salguero R, Manzanedo RD, Camarero JJ, Fernández-Cancio Á. 2014.
591 Site and age condition the growth responses to climate and drought of relict *Pinus nigra* subsp.
592 *salzmannii* populations in southern Spain. *Tree-Ring Res* 70:145–55.
- 593 Novick KA, Ficklin DL, Stoy PC, Williams CA, Bohrer G, Oishi AC, Papuga SA, Blanken PD,
594 Noormets A, Sulman BN, Scott RL, Wang L, Phillips RP. 2016. The increasing importance of
595 atmospheric demand for ecosystem water and carbon fluxes. *Nat Clim Change* 6:1023–7.
- 596 Ols C, Hofgaard A, Bergeron Y, Drobyshev I. 2016. Previous growing season climate controls the
597 occurrence of black spruce growth anomalies in boreal forests of Eastern Canada. *Can J Res*
598 46:696–705.
- 599 Pan Y, Chen JM, Birdsey R, McCullough K, He L, Deng F. 2011. Age structure and disturbance
600 legacy of North American forests. *Biogeosciences* 8:715–32.
- 601 Paré D, Bernier P, Lafleur B, Titus BD, Thiffault E, Maynard DG, Guo X. 2013. Estimating stand-
602 scale biomass, nutrient contents, and associated uncertainties for tree species of Canadian
603 forests. *Can J Res* 43:599–608.
- 604 R Core Team. 2015. R: A language and environment for statistical computing. *R Found Stat Comput*
605 Vienna Austria IURL [HttpwwwR-Proj](http://www.R-project.org). <http://www.R-project.org>.

Shifts in tree growth sensitivity to climate

- 606 Raulier F, Bernier PY, Ung C-H. 2000. Modeling the influence of temperature on monthly gross
607 primary productivity of sugar maple stands. *Tree Physiol* 20:333–45.
- 608 Régnière J, Saint-Amant R, Béchard A. 2014. BioSIM 10 — user’s manual. Rep. LAU-X-134E,
609 Natural Resources Canada, Canadian Forest Service, Laurentian Forestry Centre, Quebec, QC.
610 <https://cfs.nrcan.gc.ca/publications?id=34818>
- 611 Rennenberg H, Loreto F, Polle A, Brilli F, Fares S, Beniwal RS, Gessler A. 2006. Physiological
612 responses of forest trees to heat and drought. *Plant Biol* 8:556–71.
- 613 Robitaille A, Saucier J-P. 1998. Paysages régionaux du Québec méridional. Les Publications du
614 Québec, Québec
- 615 Rossi S, Deslauriers A, Anfodillo T, Carrer M. 2008. Age-dependent xylogenesis in timberline
616 conifers. *New Phytol* 177:199–208.
- 617 Ryan MG. 1991. Effects of climate change on plant respiration. *Ecol Appl* 1:157–67.
- 618 Schneider U, Becker A, Finger P, Meyer-Christoffer A, Rudolf B, Ziese M. 2015. GPCP Full Data
619 Reanalysis Version 7.0 at 0.5°: Monthly Land-Surface Precipitation from Rain-Gauges built
620 on GTS-based and Historic Data.
- 621 Smith NG, Malyshev SL, Shevliakova E, Kattge J, Dukes JS. 2016. Foliar temperature acclimation
622 reduces simulated carbon sensitivity to climate. *Nat Clim Change* 6:407–11.
- 623 Terrier A, Girardin MP, Périé C, Legendre P, Bergeron Y. 2013. Potential changes in forest
624 composition could reduce impacts of climate change on boreal wildfires. *Ecol Appl* 23:21–35.
- 625 Trujillo E, Molotch NP, Goulden ML, Kelly AE, Bales RC. 2012. Elevation-dependent influence of
626 snow accumulation on forest greening. *Nat Geosci* 5:705–9.
- 627 Vaganov EA, Hughes MK, Kirilyanov AV, Schweingruber FH, Silkin PP. 1999. Influence of snowfall
628 and melt timing on tree growth in subarctic Eurasia. *Nature* 400:149–51.
- 629 Viereck LA, Johnston WF. 1990. *Picea mariana* (Mill.) B. S. P., edited by: Burns, R. M. and Honkala,
630 B. H.: Silvics of North America, Vol. 1, Conifers. U.S.D.A. Forest Service Agriculture
631 Handbook 654, Washington, DC, 1990.
- 632 Vlam M, Baker PJ, Bunyavejchewin S, Zuidema PA. 2014. Temperature and rainfall strongly drive
633 temporal growth variation in Asian tropical forest trees. *Oecologia* 174:1449–61.

Shifts in tree growth sensitivity to climate

- 634 Wang Y, Hogg EH, Price DT, Edwards J, Williamson T. 2014. Past and projected future changes in
635 moisture conditions in the Canadian boreal forest. *Chron* 90:678–91.
- 636 Whitlock MC. 2005. Combining probability from independent tests: the weighted Z-method is
637 superior to Fisher’s approach: Combining probabilities from many tests. *J Evol Biol* 18:1368–
638 73.
- 639 Wilson R, D’Arrigo R, Buckley B, Büntgen U, Esper J, Frank D, Luckman B, Payette S, Vose R,
640 Youngblut D. 2007. A matter of divergence: Tracking recent warming at hemispheric scales
641 using tree ring data. *J Geophys Res* 112:D17103.
- 642 Wu X, Liu H, Guo D, Anenkhonov OA, Badmaeva NK, Sandanov DV. 2012. Growth decline linked
643 to warming-induced water limitation in Hemi-Boreal forests. *Plos One* 7.
644 [http://www.scopus.com/inward/record.url?eid=2-s2.0-](http://www.scopus.com/inward/record.url?eid=2-s2.0-84865061763&partnerID=40&md5=1de1d4dfad55bd549e297ddd5f8c15d5)
645 [84865061763&partnerID=40&md5=1de1d4dfad55bd549e297ddd5f8c15d5](http://www.scopus.com/inward/record.url?eid=2-s2.0-84865061763&partnerID=40&md5=1de1d4dfad55bd549e297ddd5f8c15d5)
- 646 Wu Z, Ahlström A, Smith B, Ardö J, Eklundh L, Fensholt R, Lehsten V. 2017. Climate data induced
647 uncertainty in model-based estimations of terrestrial primary productivity. *Environ Res Lett*
648 12:064013.
- 649 Zang C, Biondi F. 2015. treeclim: an R package for the numerical calibration of proxy-climate
650 relationships. *Ecography* 38:431–6.
- 651
- 652

653 Figure legends

654

655 **Figure 1.** (a) Location of the black spruce forests under study, eastern Canada. The sampling sites ($n =$
656 50) are shown accordingly with the positioning of transects along the west to east gradient (*colored*
657 *symbols*). Slopes of linear trends ($^{\circ}\text{C}$ per year) in summer (June to August) mean daily maximum
658 temperatures from 1901 to 2013 are shown in background colors. (b) Distribution of sampling sites
659 within gradients of mean annual temperature (MAT; $^{\circ}\text{C}$) and mean annual precipitation total (MAP;
660 mm). The CRU TS 3.22 database (Harris, Jones, Osborn, & Lister, 2014) was used for generating this
661 climate information.

662

663 **Figure 2.** Average correlations between monthly climate data and (a) RWI and (b) NPP metrics across
664 all sites over 1908-2013. Analyses were conducted using 21-yr moving windows incremented by 5
665 years. (c) Comparison of the distributions of correlations obtained in (a) and (b), for each month and
666 period combinations, using a Wilcoxon-Mann-Whitney test. Monthly climate variables included
667 minimum (Tmin) and maximum (Tmax) temperatures, and total precipitation (Prec) extracted at site
668 level from the $0.5^{\circ} \times 0.5^{\circ}$ CRU database (Harris and others 2014). Months spanned from May the year
669 previous to growth to August of the current year. Current year months start with a capital letter. The
670 significance of each averaged correlation across sites was evaluated under two sets of climate-growth
671 hypotheses using one-sided competitive tests (see 2.7 Climate-growth relationships). Open circles and
672 black dots on panels (a) and (b) identify significant ($p < 0.05$) correlations under hypotheses 1-3 and
673 4-6, respectively. Black dots on panel (c) stand for no significant ($p > 0.05$) differences in the
674 distribution of correlations.

675

676 **Figure 3.** (a) Mean of site RWI chronologies above 51.5°N . (b) Mean July to September river flow
677 measured at the De Pontois river station (53°N - 74°W , Table S3) over 1960-1993. (c) Biplot of the De
678 Pontois river flow of the year previous to growth and RWI of the year contemporaneous to growth
679 over 1961-1994. A linear regression with 95% confidence interval is shown: $R^2=0.24$. (d) Site-specific
680 correlation between De Pontois river flow and RWI. Blue and red circles represent negative and

Shifts in tree growth sensitivity to climate

681 positive correlations, respectively; the larger the circle, the higher the correlation value. Black
682 contours indicate significant correlations ($p < 0.05$).

683

684 **Figure 4.** (a) Average tree-ring width indices (black line) and net primary production (red line)
685 chronologies across all sites ($n = 50$) over 1908-2013. (b) Moving correlations between both metrics
686 were computed using 21-yr windows incremented by one year. Correlations are plotted on the central
687 year of each interval. Significant correlations ($p < 0.05$) are indicated with black dots.

688

689 **Figure 5.** Pearson correlations between site-specific RWI and NPP metrics during five different 21-yr
690 periods: (a) 1913-1933, (b) 1933-1953, (c) 1953-1973, (d) 1973-1993, and (e) 1993-2013. Correlations
691 were computed using original (left-hand panels) and first-differenced (right-hand panels) metrics. Blue
692 and red circles represent negative and positive correlations, respectively. The larger the circle, the
693 higher the correlation value ($|r|$). Black contours delineating circles indicate significant correlations (p
694 < 0.05). Black crosses indicate the position of meteorological stations available for that period.

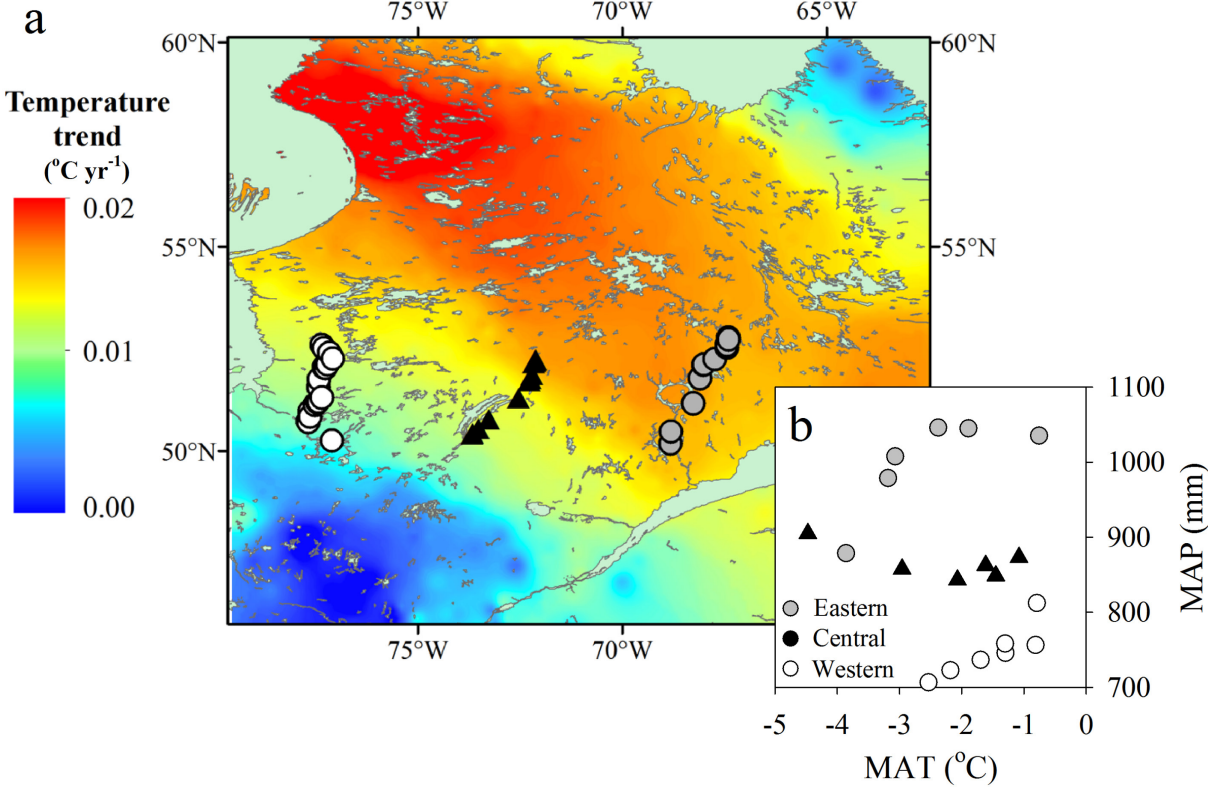
695

696 **Figure 6.** Potential factors involved in the low RWI-NPP correlation from 1953 to 1993. (a) Changes
697 in the median distances of weather stations closest to the sampling site over the years (blue:
698 precipitation; red: temperature), with 95% confidence intervals computed from exact bootstrap
699 resampling. Lower values denote a densification of the weather station network; higher values denote
700 a scarce weather station network. (b) Vertical bars: percentage of sites located within a defoliated
701 polygon of Quebec's provincial annual surveys covering 1967 to 2006 (source: MFFPQ 2014); the
702 inset map shows the projected defoliated areas from 1974 to 1978 (gray shading) relative to the
703 position of the sampling sites (black dots). Classes denote the percentage of needle loss on the annual
704 shoot: light (1 to 35%), moderate (36 to 70%), and severe (71 to 100%). (c) Site-specific altitude (alt.,
705 above sea level) against the standard deviation (SD) of the altitudinal gradients between the four
706 nearest weather stations and each site, as estimated using the software BioSIM over 1953-1993
707 (Régnière and others 2014). If the four nearest stations didn't all present climate records over the
708 entire period, additional stations were added until the full period was covered. Site-specific 1953-1993

Shifts in tree growth sensitivity to climate

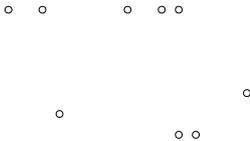
709 RWI-NPP correlations are plotted using transect-specific symbols: circles for West, squares for
710 Central and triangles for East. Blue and red symbols represent negative and positive correlations,
711 respectively; the larger the symbol, the higher the correlation value. Black contours indicate
712 significant correlations ($p < 0.05$). (d) Altitudinal gradient (map) versus the distribution of the 1953-
713 1993 NPP-RWI correlations (Jarvis and others 2008). The larger the circle, the higher the correlation
714 value. Note that the altitudinal scale was truncated to 800m to enhance contrasts between low and
715 high-altitude sampling sites.
716

Shifts in tree growth sensitivity to climate



717

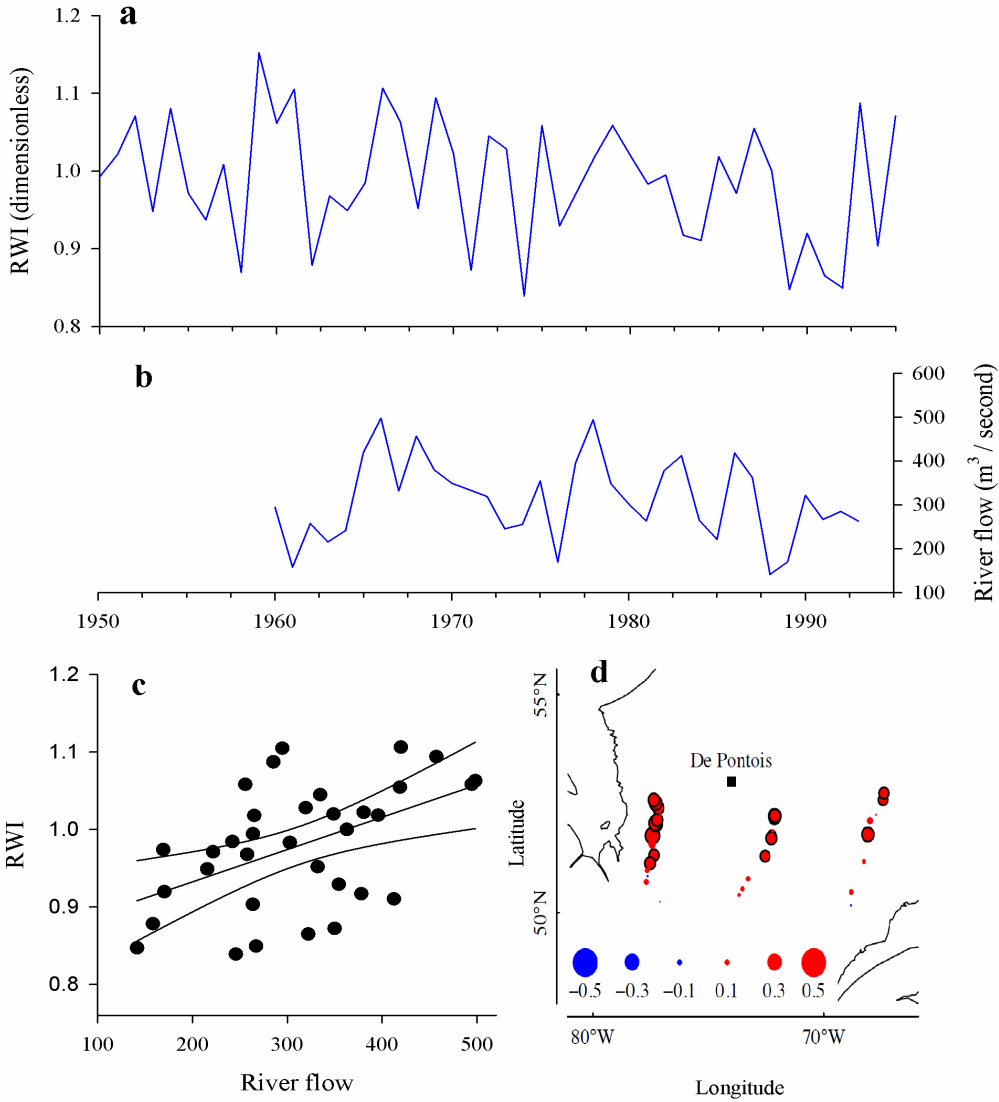
718 **Figure 1.**



719

720 **Figure 2.**

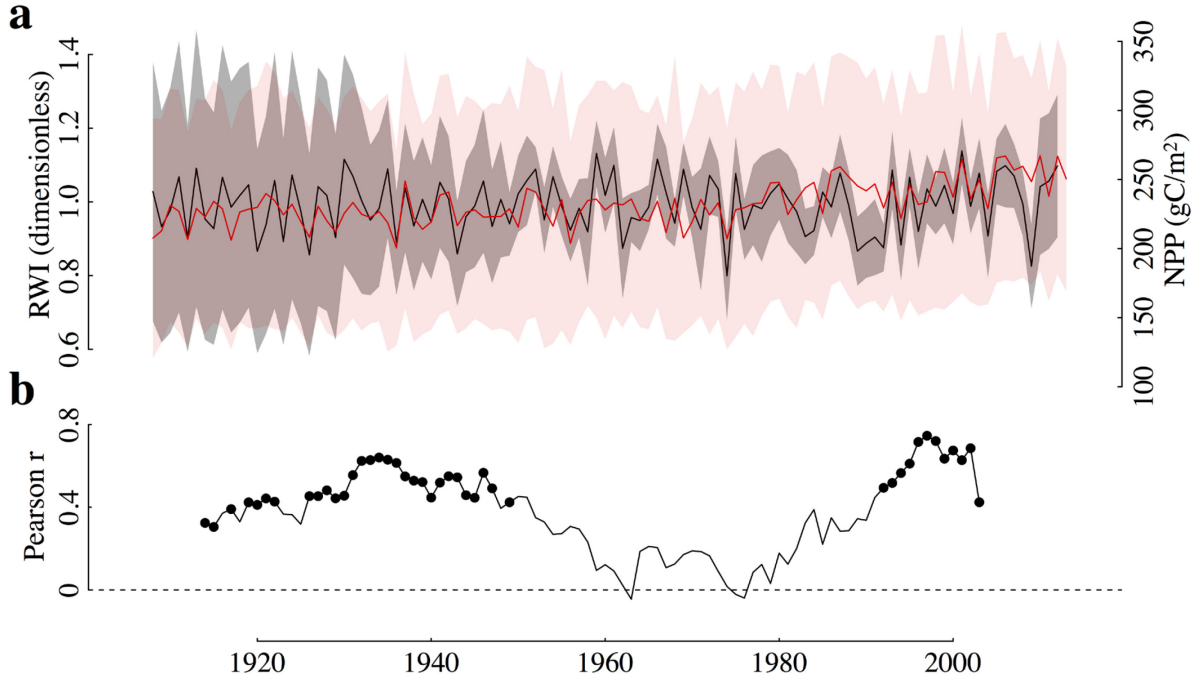
Shifts in tree growth sensitivity to climate



721

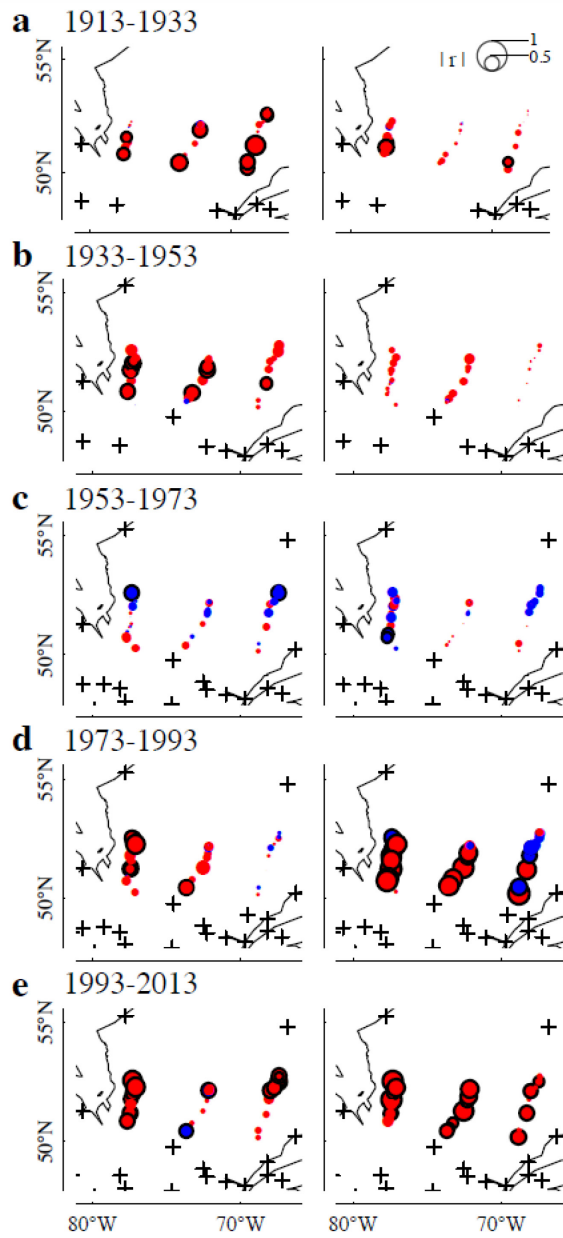
722 **Figure 3.**

Shifts in tree growth sensitivity to climate



723

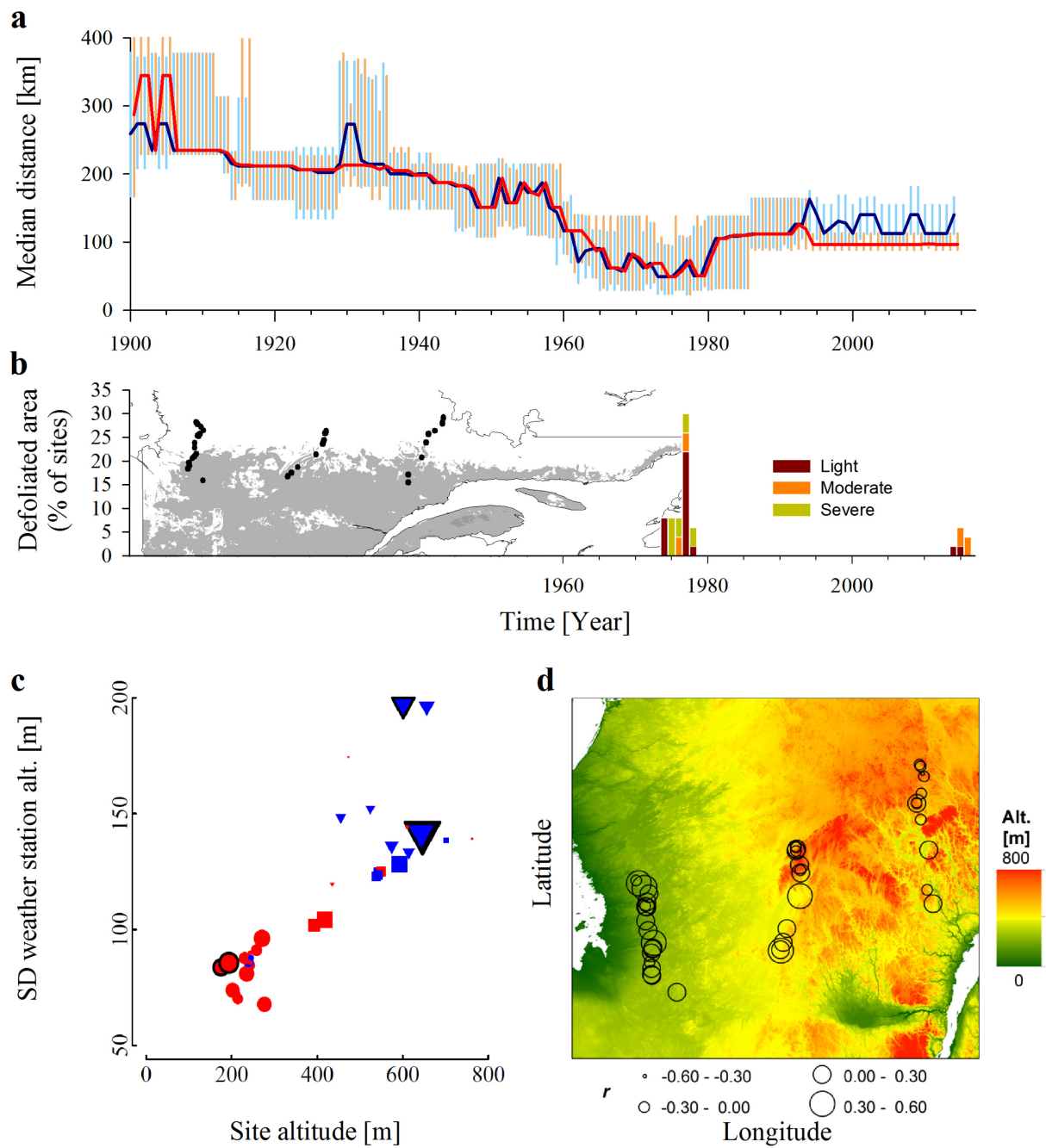
724 **Figure 4.**



725

726 **Figure 5.**

Shifts in tree growth sensitivity to climate



727

728 **Figure 6.**